Extremely efficient acceptance-rejection method for simulating uncorrelated Nakagami fading channels

David Luengo, *Member, IEEE,* Luca Martino, *Member, IEEE,*

Abstract

Multipath fading is one of the most common distortions in wireless communications. The simulation of a fading channel typically requires drawing samples from a Rayleigh, Rice or Nakagami distribution. The Nakagami-m distribution is particularly important due to its good agreement with empirical channel measurements, as well as its ability to generalize the well-known Rayleigh and Rice distributions. In this paper, a simple and extremely efficient rejection sampling (RS) algorithm for generating independent samples from a Nakagami-m distribution is proposed. This RS approach is based on a novel hat function composed of three pieces of well-known densities from which samples can be drawn easily and efficiently. The proposed method is valid for any combination of parameters of the Nakagami distribution, without any restriction in the domain and without requiring any adjustment from the final user. Simulations for several parameter combinations show that the proposed approach attains acceptance rates above 90% in all cases, outperforming all the RS techniques currently available in the literature.

Index Terms

Multipath fading, Nakagami random variables, rejection sampling.

I. Introduction

The Nakagami-m probability density function (PDF) was proposed in 1960 by Nakagami as an empirical model for the amplitude of the received samples in wireless radio communications

This work has been partly financed by the Spanish government, through the DEIPRO project (TEC2009-14504-C02-01) and the CONSOLIDER-INGENIO 2010 program (CSD2008-00010).

D. Luengo is with the Departamento de Ingeniería de Circuitos y Sistemas, Universidad Politécnica de Madrid, 28031 Madrid, Spain (e-mail:luengod@ieee.org).

L. Martino is with the Departamento de Teoría de la Señal y Comunicaciones, Universidad Carlos III de Madrid, 28911 Leganés (Madrid), Spain (e-mail:luca@tsc.uc3m.es).

subject to multipath fading [1]. This PDF is characterized by two parameters: the fading or shape parameter, m, which indicates the fading depth, and the average received power, Ω. Nakagami's fading model has been widely used to describe the wireless fading channel due to its good agreement with empirical channel measurements for some urban multipath environments [2], [3]. Moreover, the Nakagami PDF can be used to generalize or approximate several situations and densities common in wireless communications: worse-than-Rayleigh fading for $0.5 \leq m < 1$ [4], [5], Rayleigh fading for $m = 1$, and less severe fading (e.g., Rice fading) for $m > 1$, which corresponds to cases where a line of sight (LOS) path or a specular component exists, with no fading at all when $m \to \infty$. Furthermore, for $m > 1$ the Nakagami PDF is a very good approximation of the Rice density with a ratio between the power received via the LOS path to the power contribution of NLOS paths given by $K = [m - \sqrt{m(m-1)}]/\sqrt{m(m-1)}$, and can even be used to approximate the log-normal PDF (widely used to simulate shadowing) with a small σ over a specific domain. For this reason, obtaining an efficient algorithm for drawing samples from a Nakagami distribution is extremely important for the simulation and characterization of wireless channels.

On the one hand, several schemes for simulating the correlated Nakagami fading channel have been proposed [6]–[10], but all of them present limitations that may restrict their use in some practical situations. For instance, the decomposition method proposed in [6] is valid for arbitrary values of m, but it becomes inaccurate when $m \neq n/2$, with $n \in \mathbb{N}$. More accurate methods have been proposed by Yip et al. [7] as well as Beaulieu and Cheng [8], but the first one is only valid for $m < 1$, whereas the second one requires a different set of coefficients for each value of m, determined numerically or through curve fitting. More recently, a new cumulative distribution function (CDF) mapping approach based on the inverse discrete Fourier transform (IDFT) has been proposed [9], as well as a novel generation method for the spatially and temporally correlated multiple-input multiple-output (MIMO) fading channel [10]. However, all of the previous schemes focus on the generation of correlated Nakagami random variables (RVs) and their computational cost is excessive for generating independent Nakagami RVs.

On the other hand, the generation of independent Nakagami RVs is also frequently required, e.g., to simulate the performance of channel estimators, systems operating under slow fading con-

ditions or independent fading branches in diversity systems [11]. Moreover, several approaches for the generation of bivariate or multivariate Nakagami random variables (RVs) are based on drawing a sequence of independent samples first and then performing some transformation [10], [12]. Independent Nakagami RVs can be generated from Gaussian random variables, but this direct or brute force approach [13], based on the squared root of the sum of squares of n zero-mean identically distributed Gaussian RVs, is only valid when $m = n/2$, with $n \in \mathbb{N}$. Hence, several simple acceptance-rejection methods using different *hat functions* with increasing accuracy have been recently proposed [11], [14]–[16].[1] Currently, the best results for an arbitrary value of m and Ω are provided by [15] using a Gaussian PDF as the hat density. This approach achieves acceptance rates close to one for small values of m, that fall down to 70% for $m \geq 4$ without truncation and 80% truncating the hat density in the range $[0, 4\Omega]$. Unfortunately, this truncation prevents their approach from drawing samples from the tail of the Nakagami PDF, which can be important for some applications, such as co-channel interference problems [8].

In this paper we build on this work, designing an extremely efficient acceptance-rejection method for Nakagami RVs using a piecewise monotonic hat function composed of three different pieces: two truncated Gaussian PDFs and a decaying exponential PDF. The resulting hat density is based on well-known PDFs, from which samples can be easily and efficiently drawn [19], is valid for arbitrary average power and fading factors, and provides a very good fit of the target PDF, obtaining acceptance rates above 90% in all cases, which are the best ones ever reported in the literature. Furthermore, unlike previous approaches (e.g., [11], [15]), we attain this high acceptance rate without any truncation (i.e., drawing samples from the newly proposed hat density provides truly Nakagami RVs) and without requiring any adjustment from the final user (i.e., the algorithm proceeds automatically once the parameters of the Nakagami distribution are provided).

The rest of the paper is organized as follows. First of all, Section II briefly reviews the standard RS algorithm and the Nakagami PDF, introducing the novel hat function. Then, Section III

[1] In the rejection sampling literature, the normalized counterpart of the hat function is also known as the *trial*, *instrumental* or *proposal density* [17], [18]. In the sequel we will always use the term *hat function* when referring to the unnormalized version and *hat density* or *PDF* when dealing with the normalized one.

details the construction of the hat function and the procedure followed to draw samples from its normalized counterpart, and provides a lower bound for the acceptance probability. Section IV shows numerical results for several parameters of the Nakagami target PDF. Finally, Section V provides the conclusions and future lines.

II. Acceptance-Rejection Algorithm for Nakagami Random Variables

A. Rejection Sampling

Rejection sampling (RS) is a classical technique for generating samples from an arbitrary target PDF, $p_o(x) = C_p p(x)$, known up to a normalizing or proportionality constant C_p, using an alternative simpler hat PDF, $\widetilde{\pi}(x) = C_\pi \pi(x)$, such that $K\pi(x) \geq p(x)$ for some $K > 0$. RS works by drawing samples from the hat density, $x' \sim \pi(x)$,[2] and accepting or rejecting them on the basis of the ratio $p(x')/[K\pi(x')]$. The *standard RS algorithm*, which allows us to draw samples exactly from the target PDF, is the following [18]:

1) Draw $x' \sim \pi(x)$ and $w' \sim \mathcal{U}([0, 1])$.
2) If $w' \leq \frac{p(x')}{K\pi(x')}$, then x' is accepted. Otherwise, x' is discarded.
3) Repeat steps 1–2 until the desired number of samples has been obtained from the target.

The key performance measure for RS is the *mean acceptance rate* (i.e., the average number of candidate samples accepted out of the total number of samples generated), η_a, which depends on how close the hat density is to the target PDF, as shown in Section III-D. The acceptance rate determines the efficiency of an RS algorithm, since the number of samples required on average to obtain N valid samples is $N_a = N/\eta_a$. Hence, low values of η_a lead to a large number of samples being required on average, thus wasting time and computational resources.

B. Nakagami Target PDF

In this work we concentrate on developing an extremely efficient RS algorithm for generating independent unidimensional Nakagami-m random variables. The Nakagami target PDF is

[2]The notation $x' \sim \pi(x)$ will be used to denote that x' is a sample from a random variable distributed according to a proper PDF, $\pi_o(x) \propto \pi(x)$, regardless of whether $\pi(x)$ is normalized (i.e., the integral of $\pi(x)$ over its whole domain is one) or not.

$p_o(x) = C_p\ p(x)$, with normalizing constant

$$C_p = \frac{2m^m}{\Omega^m \Gamma(m)}, \tag{1}$$

and unnormalized target function

$$p(x) = x^{2m-1} \exp\left(-\frac{mx^2}{\Omega}\right) \qquad \text{for} \quad x \geq 0, \tag{2}$$

where $\Gamma(x)$ indicates the gamma function [20], $\Omega = \mathrm{E}\{x^2\} > 0$ (with $\mathrm{E}\{\cdot\}$ denoting the mathematical expectation) represents the average received power, and $m = \Omega^2/\mathrm{Var}\{x^2\} \geq 0.5$ with ($\mathrm{Var}\{\cdot\}$ denoting the variance) is a fading parameter that characterizes the fading depth of the channel; the smaller the value of m the higher the fading depth.

C. Hat Density

For the hat density we consider a simple piecewise monotonic approximation composed of three PDFs from which samples can be easily drawn. The motivation behind this hat function comes from the shape of the Nakagami PDF, which can be seen in Figure 3. On the one hand, the Nakagami target PDF is unimodal, but asymmetric w.r.t. the mode. Thus, we use two different pieces for the hat PDF on the left and right hand side of its mode in order to better accommodate the different decay rates of the target on both sides. On the other hand, providing a good hat density for the tail is critical in order to obtain a good acceptance probability [19]. Hence, we introduce a third piece of the hat PDF that provides a good fit of the target as $x \to \infty$. From Figure 3, it can be seen that the number of intervals (three) is not arbitrarily chosen, but corresponds to the natural choice given the shape of the target, thus providing the optimal trade-off between performance and computational cost. The full hat PDF is then given by $\widetilde{\pi}(x) = C_\pi \pi(x)$, with

$$\pi(x) = \pi_1(x)\mathbb{I}_1(x) + \pi_2(x)\mathbb{I}_2(x) + \pi_3(x)\mathbb{I}_3(x), \tag{3}$$

where $\pi_i(x)$ $(1 \leq i \leq 3)$ belong to the exponential class of functions,

$$\pi_i(x) = \beta_i \exp\left(-\alpha_i (x - \mu_i)^{\gamma_i}\right), \tag{4}$$

and $\mathbb{I}_i(x)$ $(1 \leq i \leq 3)$ are indicator functions, that determine whether x belongs to the interval $E_i = [e_{i-1}, e_i)$ or not, i.e.,

$$\mathbb{I}_i(x) = \begin{cases} 1, & x \in E_i, \\ 0, & x \notin E_i. \end{cases} \tag{5}$$

The intervals used for the target PDF are the left hand side of the mode, $E_1 = [0, e_1)$, its right hand side, $E_2 = [e_1, e_2)$, and the tail, $E_3 = [e_2, \infty)$. In the first two intervals, we use a truncated Gaussian density (i.e., $\gamma_1 = \gamma_2 = 2$), whereas in the third interval we use a decaying exponential (i.e., $\gamma_3 = 1$). The determination of the interval limits (e_1 and e_2), the remaining parameters (α_i, β_i and μ_i for $1 \leq i \leq 3$), and the normalizing constant, C_π, in such a way that we obtain a suitable hat function for $K = 1$ (i.e., $\pi(x) \geq p(x)$) is detailed in the following section.

III. Hat Density: Construction and Sampling

A. Hat PDF around the mode

First of all, note that, since the first two pieces of the hat PDF are two truncated Gaussian densities defined in $E_1 = [0, e_1)$ and $E_2 = [e_1, e_2)$, the optimum choice for e_1 is clearly the mode of the Nakagami target PDF. Differentiating $p(x)$ and equating it to zero, it is straightforward to show that this mode is given by

$$x_{\max} = \sqrt{\frac{\Omega(2m-1)}{2m}}, \tag{6}$$

and we set $e_1 = x_{\max}$. Then, in order to have $\pi(x)$ as close as possible to $p(x)$ within E_1 and E_2, while ensuring that $\pi(x) \geq p(x)$, we must have $\pi_1(x_{\max}) = \pi_2(x_{\max}) = p(x_{\max})$. This implies setting $\mu_1 = \mu_2 = x_{\max}$ and

$$\beta_1 = \beta_2 = p(x_{\max}) = \exp\left(-\frac{2m-1}{2}\right)\left(\frac{\Omega(2m-1)}{2m}\right)^{\frac{2m-1}{2}}. \tag{7}$$

Finally, in order to specify completely the hat function within the first two intervals we need to determine α_1 and α_2. This can be easily done by noting that, $\pi(x) \geq p(x)$ within E_1 and E_2 implies that

$$\ln \pi_i(x) = \ln p(x_{\max}) - \alpha_i (x - x_{\max})^2 \geq \ln p(x), \tag{8}$$

for any $x \in E_i$ with $i \in \{1, 2\}$. Hence, in order to obtain a valid hat function we must choose

$$\alpha_i \leq L(x), \tag{9}$$

for any $x \in E_i$ with $i \in \{1, 2\}$, and

$$L(x) = \frac{1}{(x - x_{\max})^2} \ln \frac{p(x_{\max})}{p(x)} = \frac{(2m-1)\ln(x_{\max}/x)}{(x - x_{\max})^2} + \frac{m}{\Omega} \frac{x + x_{\max}}{x - x_{\max}}. \tag{10}$$

It is easy to check that $L(x)$ is a strictly decreasing function, with $L(0) \to \infty$ and $L_\infty = \lim_{x\to\infty} L(x) = m/\Omega$. Therefore, in order to obtain the best possible fit between the hat and the target PDFs (while ensuring that $\pi(x) \geq p(x)$) within the range covered by each piece of the hat function, we must set $\alpha_1 = L(e_1)$ and $\alpha_2 = L(e_2)$. Regarding α_1, and recalling that $e_1 = x_{\max}$, with $x_{\max}$ given by (6), it can be obtained explicitly as

$$\alpha_1 = \lim_{x\to x_{\max}} L(x) = \lim_{x\to x_{\max}} \frac{(2m-1)[\ln x_{\max} - \ln x] + \frac{m}{\Omega}(x^2 - x_{\max}^2)}{(x - x_{\max})^2}. \tag{11}$$

Applying L'Hôpital's rule twice to remove the indeterminacies in this limit, (11) becomes

$$\alpha_1 = \lim_{x\to x_{\max}} \frac{-\frac{2m-1}{x} + \frac{2mx}{\Omega}}{2(x - x_{\max})} = \lim_{x\to x_{\max}} \frac{2m-1}{2x^2} + \frac{m}{\Omega} = \frac{2m}{\Omega}.$$

With respect to α_2, it is obtained similarly, evaluating $L(x)$, as given by (10), at $x = e_2$:

$$\alpha_2 = L(e_2) = \frac{1}{(e_2 - x_{\max})^2} \ln \frac{p(x_{\max})}{p(e_2)}, \tag{12}$$

with e_2 given by (20), as discussed in the sequel. Note that the conditions for α_i, given by (9) and (10), were derived in [15]. However, in [15] a single Gaussian is used for the hat function, $\pi(x) = p(x_{\max}) \exp(-\alpha(x - x_{\max})^2)$. Hence, in order to obtain a valid hat density they need to set $\alpha = L_\infty = m/\Omega$, thus achieving a much looser fit of the target and lower acceptance rates. In order to improve the efficiency of their approach, they propose to truncate the target PDF within the range $[0, 4\Omega]$. This allows them to use $\alpha = L(4\Omega)$, thus improving the efficiency of the RS approach at the expense of generating truncated Nakagami random variables, which may produce misleading results in the simulation of wireless communication channels, especially for large values of m and small values of Ω. As an alternative, here we introduce a third piece in the hat function that allows us to attain higher acceptance rates without resorting to truncation.

B. Hat PDF for the tail

The last piece, the truncated exponential PDF, is used to obtain a good approximation of the tail of the Nakagami target PDF. The hat function considered is based on the fact that

$$V(x) = \ln p(x) = (2m-1)\ln x - \frac{m}{\Omega}x^2, \tag{13}$$

is convex for any $m \geq 0.5$ and $\Omega > 0$, since $\ddot{V}(x) = -\frac{2m-1}{x^2} - \frac{2m}{\Omega} < 0$ for $x \geq 0$, with $\ddot{V}(x)$ denoting the second derivative of $V(x)$. Furthermore, setting $\beta_3 = 1$ we have $\ln \pi_3(x) = -\alpha_3(x-\mu_3)$ for $x \geq e_2$, and we can guarantee that $\pi_3(x) \geq p(x)$ for $x \geq e_2$ simply by adjusting $\ln \pi_3(x)$ to become the tangent line to $V(x)$ at $x = e_2$. It is straightforward to show that this tangent line is obtained setting

$$\alpha_3 = -\dot{V}(e_2) = -\frac{2m-1}{e_2} + \frac{2m}{\Omega}e_2, \tag{14}$$

with $\dot{V}(e_2)$ indicating the first derivative of $V(x)$ evaluated at $x = e_2$, and

$$\alpha_3\mu_3 = V(e_2) - \dot{V}(e_2)e_2 = (2m-1)(\ln e_2 - 1) + \frac{m}{\Omega}e_2^2, \tag{15}$$

so that finally

$$\mu_3 = \frac{(2m-1)(\ln e_2 - 1) + \frac{m}{\Omega}e_2^2}{\frac{2m-1}{e_2} - \frac{2m}{\Omega}e_2}. \tag{16}$$

The last element required for the complete definition of the hat density is the limit between the second and third intervals, e_2. The optimum value for e_2, e_2^*, can be obtained by minimizing the discrepancy between the target and the hat function within E_2 and E_3. Since $\pi(x) \geq p(x)\ \forall x > 0$ by construction, and $p(x)$ is fixed, e_2^* is given by (see the Appendix)

$$\begin{aligned} e_2^* &= \arg\max_{e_2} \{\eta_a(e_2)\} \\ &= \arg\min_{e_2} \{A_2(e_2) + A_3(e_2)\} \\ &= \arg\min_{e_2} \left\{ \frac{p(x_{\max})}{2}\sqrt{\frac{\pi}{\alpha_2}}\text{erf}\left(\sqrt{\alpha_2}(e_2 - x_{\max})\right) + \frac{1}{\alpha_3}\exp(-\alpha_3(x-\mu_3)) \right\}, \end{aligned} \tag{17}$$

where $\eta_a(e_2)$ denotes the average acceptance rate expressed as a function of e_2, $A_2(e_2)$ and $A_3(e_2)$ are the areas of the second and third pieces of the hat function given by (23) and (24) respectively, and $\text{erf}\,(x)$ denotes the well-known error function [13], [20]:

$$\text{erf}\,(x) = \frac{2}{\sqrt{\pi}}\int_0^x \exp(-t^2)\ dt. \tag{18}$$

Unfortunately, a closed-form expression for e_2^* cannot be found, since several parameters (α_2, α_3 and μ_3) depend on e_2. An approximately optimal solution can be found numerically through grid search, but this procedure may be too complicated for practical application. However, a good sub-optimal approximation can be easily obtained by noting that:

1) The point e_2 should correspond to the beginning of the tail of the Nakagami PDF.
2) The right hand side tail of a density is necessarily convex by definition.

Therefore, we argue that e_2^* must satisfy the inequality $e_2^* \geq x_{in}$, with x_{in} denoting the largest inflection point in the Nakagami PDF, which guarantees that $p(x)$ is convex for $x > x_{in}$. This point can be easily found as the largest solution of $d^2p(x)/dx^2 = 0$ and is given by

$$x_{in} = \frac{1}{2}\sqrt{\frac{\Omega(4m + \sqrt{16m - 7} - 1)}{m}}. \tag{19}$$

Moreover, although setting $e_2 = x_{in}$ provides satisfactory results, we have found empirically that a better approximation of the optimal value e_2^* is given by

$$e_2 = \hat{e}_2^* = x_{in} + \frac{\Omega}{4m} + am^b + c, \tag{20}$$

with $a = -0.8$, $b = 0.1$ and $c = 1.2$. This approximation is simple enough to be used in practice, provides an improvement in acceptance probability of 4 – 9 % w.r.t. using $e_2 = x_{in}$ and the loss w.r.t. the approximately optimal solution derived numerically is usually less than 2 %.[3] Nevertheless, since the cost function to be minimized, $J(e_2) = A_2(e_2) + A_3(e_2)$, is convex, the optimal acceptance rate can always be attained through a gradient descent minimization algorithm [21], [22]. Mathematically, we can find an extremely close approximation to e_2^* iteratively as

$$\hat{e}_2[n+1] = \hat{e}_2[n] - \rho_n \nabla J(\hat{e}_2[n]), \tag{21}$$

where ρ_n is the step size parameter and $\nabla J(\hat{e}_2[n])$ denotes the gradient of $J(e_2)$ evaluated at $e_2 = \hat{e}_2[n]$, which is provided in the Appendix. Note that, although the expressions for this gradient are quite involved, this process has to be performed only once, during the initialization stage of the algorithm. Therefore, the increase in acceptance rate obtained may be worth the

[3]Indeed, we have only noticed differences above 2 % for very large values of Ω and small values of m, e.g., $\Omega = 100$ and $m \leq 2$, where the difference in acceptance probability can rise up to 4 % (see Figure 2).

effort when a large number of samples have to be drawn, as it often happens in the evaluation of wireless communication systems under fading conditions.

Fig. 1 shows two examples of the performance of the gradient descent algorithm using $\hat{e}_2[0] = x_{in}$ and $\rho_n = 0.2 \times 0.999^n$. In both cases the optimum value of e_2 (obtained numerically through a grid search) is attained after a moderate number of iterations (around 500 and 1600 respectively for a stopping condition $|\hat{e}_2[n+1] - \hat{e}_2[n]| < 10^{-5}$). On the one hand, in the first case the acceptance rate is only improved marginally w.r.t. using the value of e_2 given by (20) (0.02 % improvement), as shown in Fig. 2(a), so the optimization is not worth the effort. On the other hand, in the second case the acceptance rate is improved substantially w.r.t. using $e_2 = \hat{e}_2^*$ (3.85 % improvement), as shown in Fig. 2(b), so the optimization is clearly worth the effort when the number of samples to be drawn is large enough. Note that in both cases the improvement in acceptance rate of using either $e_2 = \hat{e}_2^*$ or the gradient descent w.r.t. setting $e_2 = x_{in}$ as given by (19) is remarkable: around 6.71 % in the first case and up to 7.73 % in the second one.

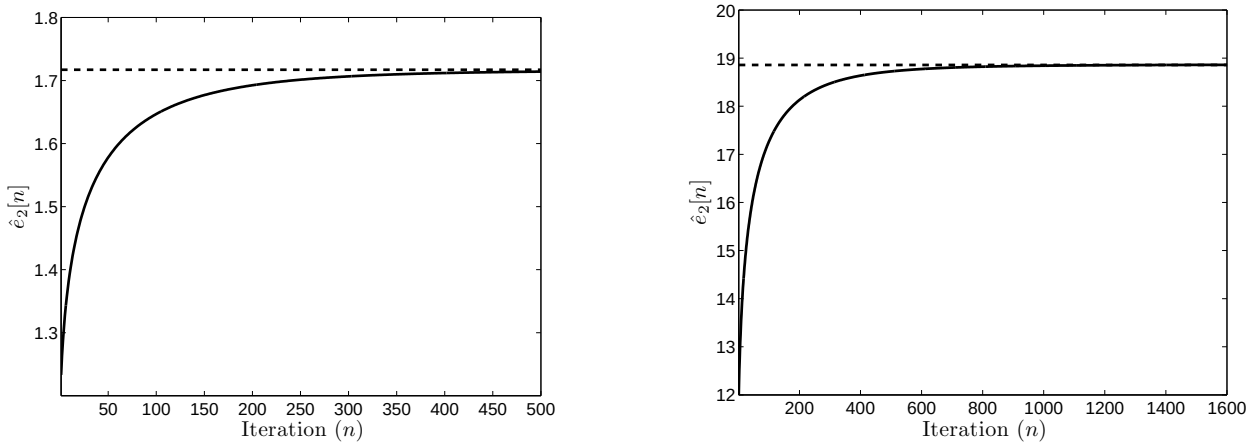

(a) (b)

Fig. 1. Convergence of the gradient descent algorithm using $\hat{e}_2[0] = x_{in}$ and $\rho_n = 0.2 \times 0.999^n$ (continuous line) to the optimum value e_2^* obtained numerically through a grid search (dashed line). **(a)** $m = 1.5$ and $\Omega = 1$. **(b)** $m = 0.8$ and $\Omega = 100$.

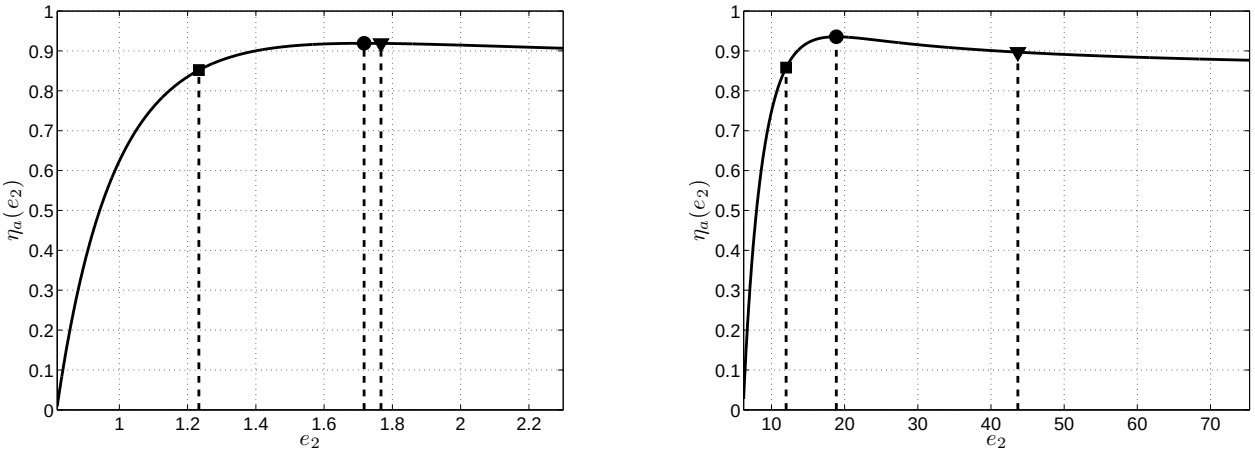

(a) (b)

Fig. 2. Average acceptance rate as a function of e_2 and acceptance rates obtained using $e_2 = x_{in}$ as given by (19) [square], $e_2 = \hat{e}_2^*$ as given by (20) [triangle] and the e_2 obtained iteratively using the gradient descent algorithm shown in (21) [circle]. **(a)** $m = 1.5$ and $\Omega = 1$. **(b)** $m = 0.8$ and $\Omega = 100$.

C. Drawing samples from the hat PDF

First of all, we recall that the unnormalized hat PDF is given by

$$\pi(x) = \begin{cases} \pi_1(x) = \beta_1 \exp(-\alpha_1(x-\mu_1)^{\gamma_1}), & 0 \leq x < e_1; \\ \pi_2(x) = \beta_2 \exp(-\alpha_2(x-\mu_2)^{\gamma_2}), & e_1 \leq x < e_2; \\ \pi_2(x) = \beta_3 \exp(-\alpha_3(x-\mu_3)^{\gamma_3}), & x \geq e_2. \end{cases} \tag{22}$$

The parameters required to construct this hat function, which have been derived in the previous sections, are summarized in Table I.[4] Note that all the parameters can be easily calculated and stored, the whole process is automatic (i.e., it can be performed automatically given the values of m and Ω, without requiring the user to adjust manually any parameter) and has to be performed only once before drawing all the samples required. As an example, Fig. 3 shows the target, $p(x)$, our hat PDF, $\pi(x)$, and the hat density used in [15] for an unbounded domain, which fits the target PDF in a much looser way, thus leading to worse acceptance rates.

[4]Note that we have used $e_2 = \hat{e}_2^*$, but this can be easily substituted by the value obtained from the gradient descent algorithm, as discussed in the previous section.

i	β_i	α_i	μ_i	γ_i	e_i
1	$x_{\max}^{2m-1}\exp\left(-\frac{mx_{\max}^2}{\Omega}\right)$	$\frac{2m}{\Omega}$	$x_{\max}$	2	$x_{\max}$
2	$x_{\max}^{2m-1}\exp\left(-\frac{mx_{\max}^2}{\Omega}\right)$	$\frac{1}{(e_2-x_{\max})^2}\ln\frac{p(x_{\max})}{p(e_2)}$	$x_{\max}$	2	$x_{in}+\frac{\Omega}{4m}-0.8m^{0.1}+1.2$
3	1	$-\frac{2m-1}{e_2}+\frac{2m}{\Omega}e_2$	$\frac{(2m-1)(\ln e_2-1)+\frac{m}{\Omega}e_2^2}{\frac{2m-1}{e_2}-\frac{2m}{\Omega}e_2}$	1	—

TABLE I

PARAMETERS REQUIRED TO CONSTRUCT THE HAT FUNCTION FOR THE REJECTION SAMPLING ALGORITHM.

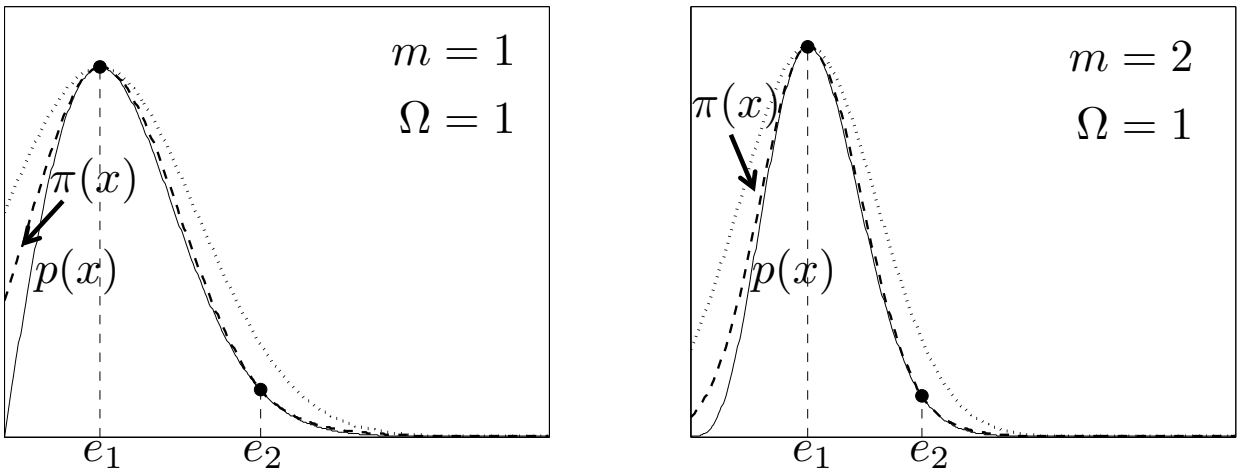

(a) (b)

Fig. 3. Target function $p(x)$ (continuous line), our hat function $\pi(x)$ (dashed line) and the hat function used in [15] for an unbounded domain (dotted line). **(a)** Construction for $m = 1$ and $\Omega = 1$. **(b)** Construction for $m = 2$ and $\Omega = 1$.

Once the hat PDF, $\pi_o(x) \propto \pi(x)$, has been defined, one of the three truncated PDFs with non-overlapping supports must be selected with probabilities proportional to their areas,[5] which can be easily obtained in a closed form. For the first region we have

$$\begin{aligned} A_1 &= \int_0^{e_1} \pi_1(x)\, dx \\ &= p(x_{\max}) \int_0^{x_{\max}} \exp(-\alpha_1 (x - x_{\max})^2)\, dx \\ &= \frac{p(x_{\max})}{2}\sqrt{\frac{\pi}{\alpha_1}}\text{erf}\left(\sqrt{\alpha_1}x_{\max}\right), \end{aligned} \tag{23}$$

[5]Let us remark that the three portions of the hat PDF are not normalized, so their areas will not be equal to one in general.

where $\text{erf}\,(x)$ denotes again the error function. Similarly, for the second region we have

$$\begin{aligned} A_2(e_2) &= \int_{e_1}^{e_2} \pi_2(x)\ dx \\ &= p(x_{\max}) \int_{x_{\max}}^{e_2} \exp(-\alpha_2(x - x_{\max})^2)\ dx \\ &= \frac{p(x_{\max})}{2}\sqrt{\frac{\pi}{\alpha_2}}\text{erf}\left(\sqrt{\alpha_2}(e_2 - x_{\max})\right), \end{aligned} \tag{24}$$

where we have emphasized the dependenc on e_2, and for the last region,

$$\begin{aligned} A_3(e_2) &= \int_{e_2}^{\infty} \pi_3(x)\ dx \\ &= \int_{e_2}^{\infty} \exp(-\alpha_3(x - \mu_3))\ dx \\ &= \frac{1}{\alpha_3}\exp(-\alpha_3(e_2 - \mu_3)). \end{aligned} \tag{25}$$

Finally, samples must be drawn from the selected piece of the hat density. For the truncated Gaussians there are many techniques available in the literature (see e.g. [23]–[25]) that allow us to draw samples efficiently. In particular, here we propose using the inversion method [23], since it can also be used to obtain samples easily and efficiently from the truncated exponential [17]–[19]. Hence, the full RS approach is the following:

1) Given m and Ω, obtain the parameters required to construct the hat function, given by (22), using Table I and the gradient descent approach to optimize e_2 if desired. Store them.
2) Compute the selection probabilities for each of the pieces of the hat function, $P_i = A_i/(A_1 + A_2 + A_3)$ for $1 \leq i \leq 3$, and store them.
3) Select the i-th interval of the hat function ($1 \leq i \leq 3$) with probability P_i.
4) Draw $x' \sim \pi_i(x)$ and $w' \sim \mathcal{U}([0, 1])$.
5) If $w' \leq \frac{p(x')}{\pi_i(x')}$, then x' is accepted. Otherwise, x' is discarded.
6) Repeat steps 3–5 until the desired number of samples has been obtained from the target.

Therefore, we need to calculate and store 8 different real numbers during the initialization stage. Then, at each iteration of the algorithm we just need to draw two uniform random variables, obtain a sample from the hat density using the inversion method and evaluate $p(x')/\pi_i(x')$. Consequently, the operations performed at each iteration of the algorithm are essentially the

same as in [15], but the acceptance rate is much higher, thus leading to an important reduction in the computational cost, as shown in Section IV.

D. Mean acceptance rate of the proposed approach

As mentioned before, the key performance issue for an RS algorithm is the acceptance probability or mean acceptance rate. In this section, we show the expressions for the acceptance probability and provide a tight lower bound for our algorithm. First of all, note that the mean acceptance rate can be expressed as

$$\begin{aligned}\eta_a(e_2) &= \int_0^\infty p_a(x)\widetilde{\pi}(x)\ dx \\ &= \int_0^\infty \frac{p(x)}{K\pi(x)}\widetilde{\pi}(x)\ dx \\ &= \frac{C_\pi(e_2)}{K}\int_0^\infty p(x)\ dx = \frac{C_\pi(e_2)}{KC_p},\end{aligned} \tag{26}$$

where $p_a(x) = \frac{p(x)}{K\pi(x)}$ denotes the probability of accepting a sample $x \sim \widetilde{\pi}(x)$, $K = 1$ by design, since we have constructed $\pi(x)$ ensuring that $\pi(x) \geq p(x)$ for any value of x, C_p is given by Eq. (1), and

$$\begin{aligned}\frac{1}{C_\pi(e_2)} &= \int_0^\infty \pi(x)\ dx \\ &= \int_0^{x_{\max}} \pi_1(x)\ dx + \int_{x_{\max}}^{e_2} \pi_2(x)\ dx + \int_{e_2}^\infty \pi_3(x)\ dx \\ &= A_1 + A_2(e_2) + A_3(e_2).\end{aligned} \tag{27}$$

Hence, the mean acceptance rate finally becomes

$$\eta_a(e_2) = \frac{C_p^{-1}}{A_1 + A_2(e_2) + A_3(e_2)}. \tag{28}$$

By setting $e_2 = e_2^*$ the optimum value of the acceptance rate, $\eta_a(e_2^*)$, would be obtained. Unfortunately, we cannot obtain an analytical expression for e_2^*, but we can easily provide a lower bound by using $e_2 = x_{in}$, with x_{in} given by (19), or $e_2 = \hat{e}_2^*$ with $\hat{e}_2^*$ given by (20). Fig. 4 displays the optimum acceptance rate and these two lower bounds as a function of m for different values of Ω, showing that $\eta_a(\hat{e}_2^*)$ is quite close to $\eta_a(e_2^*)$, especially for the frequently used normalized value $\Omega = 1$.

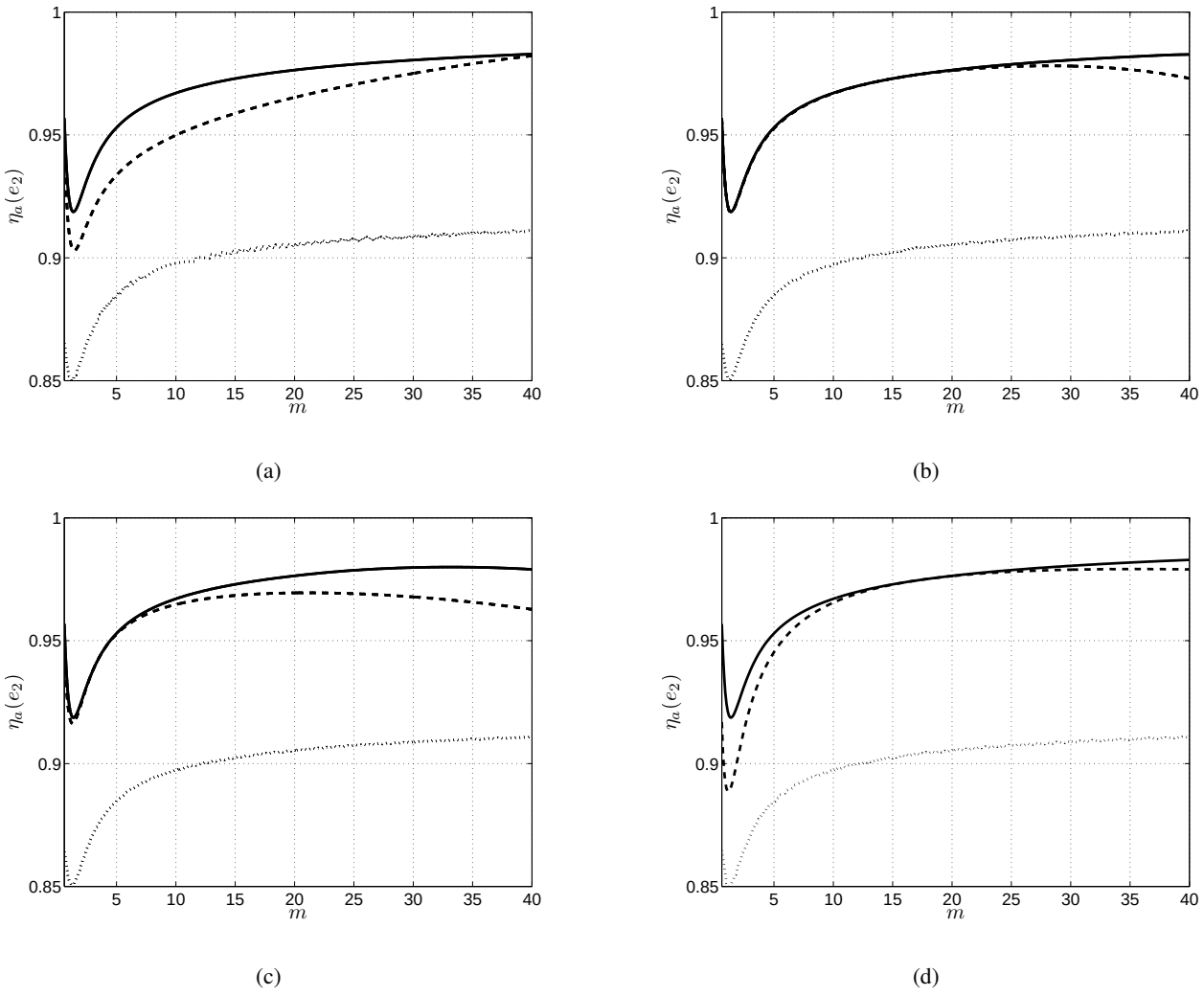

(a) (b)

(c) (d)

Fig. 4. Optimum acceptance rate $\eta_a(e_2^*)$ [continuous line] and two lower bounds, $\eta_a(x_{in})$ obtained using $e_2 = x_{in}$ [dashed line] and $\eta_a(\hat{e}_2^*)$ obtained using $e_2 = \hat{e}_2^*$ [dotted line], as a function of m for different values of Ω. **(a)** $\Omega = 0.1$. **(b)** $\Omega = 1$. **(c)** $\Omega = 10$. **(d)** $\Omega = 100$.

IV. Simulation Results

First of all, in order to analyze the performance of the proposed algorithm we have generated $N = 5 \cdot 10^5$ samples using the hat function given by (22). Fig. 5 depicts two examples of the Nakagami PDF, $p_o(x) \propto p(x)$: for $m = 0.6$ and $\Omega = 1$ in Fig. 5(a), and for $m = 2$ and $\Omega = 1$ in Fig. 5(b). Fig. 5 also displays the normalized histogram obtained using the samples generated by the RS algorithm. In both cases the histogram closely resembles the target density, both around the mode and the tails, showing that our approach is able to produce samples from the true PDF

without resorting to a truncated approximation, as required by certain methods to improve the efficiency (e.g., the ones proposed in [11], [15]). In order to confirm the good performance of our approach for the tails, Fig. 6 displays the complementary cumulative distribution function (CCDF), $\bar{F}(x) = 1 - F(x)$, for the same two examples in logarithmic scale. Fig. 6 shows the good match between the generated samples and the Nakagami CCDF, with the discrepancies for $\bar{F}(x) < 10^{-4}$ due to the limited number of samples available. Indeed, the RS algorithm guarantees that samples are drawn from the target PDF as long as $\pi(x) \geq p(x)$ for any value of x [17]–[19]. Thus, in order to obtain a better approximation of the tails, all what is required is a larger number of samples.

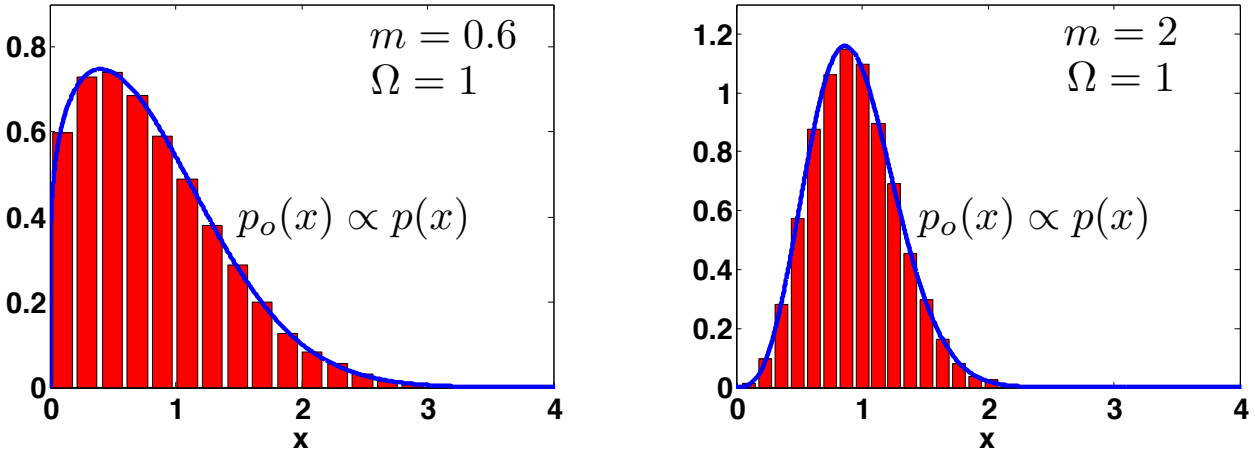

(a) (b)

Fig. 5. Normalized histogram of the generated samples ($N = 5 \cdot 10^5$) and the normalized Nagakami PDF, $p_o(x) \propto p(x)$. **(a)** $m = 0.6$, $\Omega = 1$. **(b)** $m = 2$, $\Omega = 1$.

Then we focus on the average acceptance rate (i.e., the number of samples accepted out of the total number of samples generated), which is the efficiency measure commonly used to characterize RS algorithms. Fig. 7 shows the acceptance rate for several values of the fading parameters (both as a function of m and Ω), comparing it to the approach described in [15], which is the most efficient one currently available. It can be seen that our technique is extremely efficient, providing the best results ever reported in the literature, with acceptance rates above 90% in all cases and up to 97% in some cases, whereas the efficiency of [15] falls down to 80%

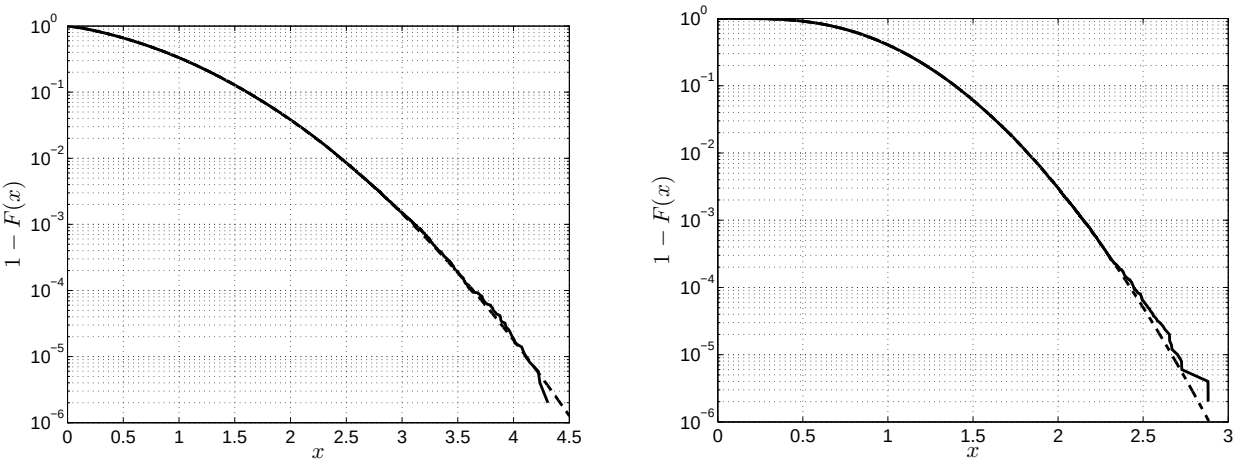

(a) (b)

Fig. 6. Empirical complementary cumulative distribution function (CCDF) obtained using $N = 5 \cdot 10^5$ (continuous line) and theoretical Nagakami CCDF (dashed line). **(a)** $m = 0.6$, $\Omega = 1$. **(b)** $m = 2$, $\Omega = 1$.

for $m \geq 4$ in the truncated case (not shown), and to 70% without truncation. This means that in order to generate N samples our approach will never need more than $1.11 \times N$ iterations on average for any combination of the fading parameters, whereas the approach in [15] will need $1.25 \times N$ iterations on average for $m \geq 4$ in the truncated case, and $1.43 \times N$ without truncation.

Finally, we note that the average acceptance rate does not provide all the information about the efficiency of the algorithm, since the generation of samples from different hat function may require different amounts of complexity. Hence, in order to provide a fair comparison with the approach of [15], which is the best RS approach currently available in the literature, Table II shows the time required to generate $N = 10^4$ samples using the hat function of [15] and the newly proposed hat function. In this case, since the samples from all the pieces in our hat function are generated using the inversion method, just like the samples from the hat function in [15] (note that their hat function is a single Gaussian truncated at $x = 0$), our approach has a similar computational cost per iteration than the approach of [15] (with the only difference due to having to select one of the three pieces). Hence, the increase in acceptance rate directly leads to a decrease in computational cost, as shown clearly in Table II, where we can see a decrease

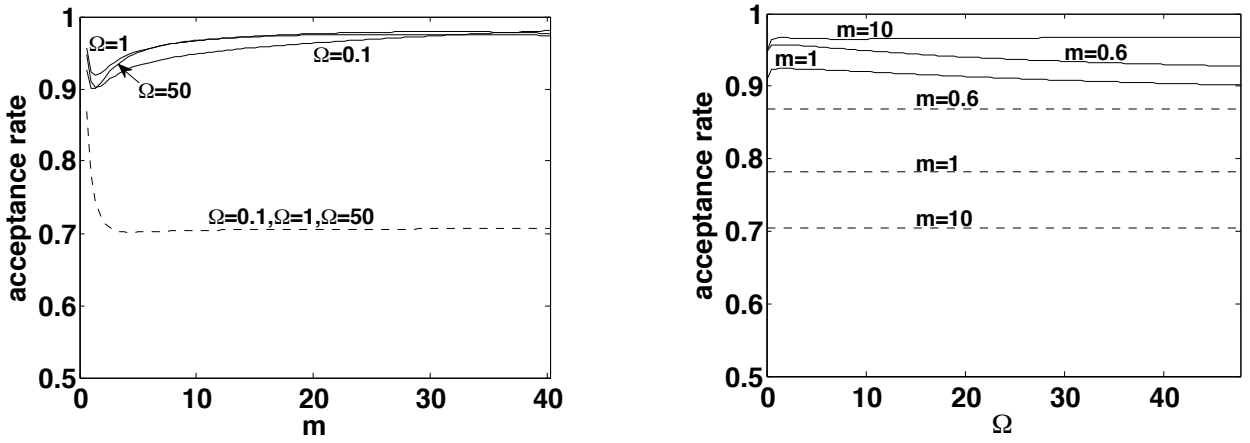

(a) (b)

Fig. 7. Acceptance rates obtained using our hat density (continuous line) and the one from [15] for an unbounded domain (dashed line). **(a)** Fixing Ω ($\Omega \in \{0.1, 1, 50\}$) and varying m. **(b)** Fixing m ($m \in \{0.6, 1, 10\}$) and varying Ω.

in the time required to draw $N = 10^4$ samples up to 28.26 % for large values of m.

m	Method from [15]	Novel Approach		
		$\Omega = 0.1$	$\Omega = 1$	$\Omega = 50$
0.6	1.0983	1.0251	0.9927	1.0509
1	1.2074	1.0670	1.0309	1.0805
2	1.3161	1.0712	1.0387	1.0658
5	1.3268	1.0442	1.0158	1.0268
10	1.3305	1.0263	1.0040	1.0035
20	1.3337	1.0139	0.9956	0.9824
40	1.3321	0.9976	0.9662	0.9556

TABLE II

COMPARISON OF THE TIME REQUIRED TO GENERATE $N = 10^4$ SAMPLES USING THE HAT FUNCTION OF [15] AND THE NEWLY PROPOSED HAT FUNCTION.

V. CONCLUSIONS AND FUTURE LINES

In this paper we have proposed an automatic rejection sampling (RS) algorithm to generate independent samples from Nakagami random variables, which are required for simulating the

Nakagami-m fading channel, with arbitrary fading parameters. Our approach is based on a novel hat density composed of three pieces: two truncated Gaussians around the mode and an exponential for the tail. The resulting algorithm is simple and extremely efficient, providing acceptance rates above 90% for any value of the fading parameters (m and Ω), which are the best ones ever reported in the literature. Furthermore, for certain values of m and Ω the proposed RS scheme attains acceptance rates up to 97%, thus providing virtually exact sampling (i.e., sampling without any rejection). Moreover, unlike some previous approaches, these high acceptance rates are obtained without any truncation of the domain (i.e., we always provide samples from the true target density) and without requiring any adjustment from the final user. Future research lines include extending the method to the generation of multiple correlated Nakagami RVs and other distributions commonly used in the simulation of fading/shadowing in wireless channels.

APPENDIX

The cost function that has to be minimized in order to obtain the optimum value of e_2, e_2^*, is

$$J(e_2) = A_2(e_2) + A_3(e_2), \tag{29}$$

where $A_2(e_2)$ and $A_3(e_2)$ are given by (24) and (25) respectively. Hence, the gradient w.r.t. e_2 is simply

$$\nabla J(e_2) = \nabla A_2(e_2) + \nabla A_3(e_2). \tag{30}$$

The first gradient in (30) is given by

$$\nabla A_2(e_2) = \frac{p(x_{\max})}{2}\sqrt{\frac{\pi}{\alpha_2}}\left[-\text{erf}\left(\sqrt{\alpha_2}(e_2 - x_{\max})\right)\frac{\nabla\alpha_2(e_2)}{2\alpha_2} + \nabla\text{erf}\left(\sqrt{\alpha_2}(e_2 - x_{\max})\right)\right], \tag{31}$$

where

$$\nabla\alpha_2(e_2) = \frac{\alpha_3(e_2) - 2\alpha_2(e_2 - x_{\max})}{(e_2 - x_{\max})^2} \tag{32}$$

and

$$\nabla\text{erf}\left(\sqrt{\alpha_2}(e_2 - x_{\max})\right) = \frac{2}{\sqrt{\pi}}\left(\frac{(e_2 - x_{\max})\nabla\alpha_2(e_2)}{2\sqrt{\alpha_2}} + \sqrt{\alpha_2}\right)\exp(-\alpha_2(e_2 - x_{\max})^2). \tag{33}$$

Regarding the second gradient, it is given by

$$\nabla A_3(e_2) = -\left(1 + \frac{\nabla\alpha_3(e_2)}{\alpha_3^2}\right)\exp(-\alpha_3(e_2 - \mu_3)), \tag{34}$$

where

$$\nabla\alpha_3(e_2) = \frac{2m-1}{e_2^2} + \frac{2m}{\Omega}. \tag{35}$$

REFERENCES

[1] M. Nakagami, "The m-distribution—a general formula of intensity distribution of rapid fading," in *Statistical Methods in Radio Wave Propagation*, W. G. Hoffman, Ed. Oxford (UK): Pergamon, 1960.

[2] H. Suzuki, "A statistical model for urban radio propagation," *IEEE Trans. on Communications*, vol. 25, no. 7, pp. 673–680, Jul. 1977.

[3] W. R. Braun and U. Dersch, "A physical mobile radio channel model," *IEEE Transactions on Vehicular Technology*, vol. 40, no. 2, pp. 472–482, May 1991.

[4] N. C. Beaulieu and A. M. Rabiei, "Linear diversity combining on Nakagami-0.5 fading channels," *IEEE Transactions on Communications*, vol. 59, pp. 2742–2752, Oct. 2011.

[5] A. Behnad, N. C. Beaulieu, and B. Maham, "Multi-hop amplify-and-forward relaying on Nakagami-0.5 fading channels," *IEEE Wireless Communications Letters*, vol. 1, pp. 173–176, June 2012.

[6] Q. T. Zhang, "A decomposition technique for efficient generation of correlated Nakagami fading channels," *IEEE Journal on Selected Areas in Communications*, vol. 18, no. 11, pp. 2385–2392, Nov. 2000.

[7] K.-W. Yip and T.-S. Ng, "A simulation model for Nakagami-m fading channels, $m < 1$," *IEEE Transactions on Communications*, vol. 48, no. 2, pp. 214–221, Feb. 2000.

[8] N. C. Beaulieu and C. Cheng, "Efficient Nakagami-m fading channel simulation," *IEEE Transactions on Vehicular Technology*, vol. 54, no. 2, pp. 413–424, Mar. 2005.

[9] Y. Ma and D. Zhang, "A method for simulating complex Nakagami-m fading time series with nonuniform phase and prescribed autocorrelation characteristics," *IEEE Trans. on Vehicular Technology*, vol. 59, no. 1, pp. 29–35, Jan. 2010.

[10] Q.-M. Zhu, X.-B. Yu, J.-B. Wang, D.-Z. Xu, and X.-M. Chen, "A new generation method for spatial-temporal correlated MIMO Nakagami fading channel," *Int. Journal of Antennas and Propagation*, p. 8 pp., 2012.

[11] L. Cao and N. C. Beaulieu, "Simple efficient methods for generating independent and bivariate Nakagami-m fading envelope samples," *IEEE Transactions on Vehicular Technology*, vol. 56, no. 4, pp. 1573–1579, Jul. 2007.

[12] C. Tellambura and A. Jayalath, "Generation of bivariate Rayleigh and Nakagami-m fading envelopes," *IEEE Communications Letters*, vol. 4, no. 5, pp. 170–172, May 2000.

[13] J. G. Proakis, *Digital Communications (4th edition)*. Singapore: McGraw-Hill, 2000.

[14] M. Matthaiou and D. Laurenson, "Rejection method for generating Nakagami-m independent deviates," *IET Electronics Letters*, vol. 43, no. 25, pp. 1474–1475, Dec. 2007.

[15] Q. Zhu, X. Dang, D. Xu, and X. Chen, "Highly efficient rejection method for generating Nakagami-m sequences," *IET Electronics Letters*, vol. 47, no. 19, pp. 1100–1101, Sep. 2011.

[16] D. Luengo and L. Martino, "Almost rejectionless sampling from nakagami-m distributions ($m \geq 1$)," *IET Electronics Letters*, vol. 48, no. 24, pp. 1559–1561, Nov. 2012.

[17] W. Hörmann, J. Leydold, and G. Derflinger, *Automatic nonuniform random variate generation*. Springer, 2003.

[18] J. E. Gentle, *Random Number Generation and Monte Carlo Methods*. New York, NY, USA: Springer, 2005.

[19] L. Devroye, *Non-Uniform Random Variate Generation*. Springer, 1986.

[20] M. Abramowitz and I. A. Stegun, Eds., *Handbook of Mathematical Functions: With Formulas, Graphs, and Mathematical Tables (10th Printing)*. New York, NY (USA): Dover, Dec. 1972.

[21] A. H. Sayed, *Adaptive Filters*. New Jersey, NJ (USA): John Wiley & Sons, 2008.

[22] S. O. Haykin, *Adaptive Filter Theory (5th Edition)*. New Jersey, NJ (USA): Prentice Hall, 2013.

[23] J. Kotecha and P. M. Djurić, "Gibbs sampling approach for generation of truncated multivariate Gaussian random variables," *Proc. IEEE Int. Acoustics, Speech, and Signal Proc. Conf., (ICASSP)*, 1999.

[24] N. Chopin, "Fast simulation of truncated Gaussian distributions," *Statistics and Computing*, vol. 21, no. 2, pp. 275–288, Dec. 2009.

[25] D. Luengo and L. Martino, "Efficient random variable generation: ratio of uniforms and polar rejection sampling," *IET Electronics Letters*, vol. 48, no. 6, pp. 326–327, March 2012.